International Dairy Journal 155 (2024) 105968

Contents lists available at ScienceDirect

International Dairy Journal

journal homepage: www.elsevier.com/locate/idairyj

Storage stability of model infant formula powders produced under varying wet-mix processing conditions

Mariana Rodríguez Arzuaga [a, *], Analía G. Abraham [b], Leopoldo Suescun [c], Alejandra Medrano [d], Lilia Ahrné [e], Marcela Díaz [f], Jessica Báez [d], María Cristina Añón [b]

[a] Latitud – LATU Foundation, Av. Italia 6201, 11500, Montevideo, Uruguay
[b] Centro de Investigación y Desarrollo en Criotecnología de Alimentos (CIDCA), Comisión de Investigaciones Científicas (CIC-PBA), Consejo Nacional de Investigaciones Científicas y Técnicas (CONICET-CCT La Plata), Universidad Nacional de La Plata (UNLP), Calle 47 y 116, La Plata, 1900, Buenos Aires, Argentina
[c] Cryssmat-Lab/DETEMA, Facultad de Química, Universidad de la República, Av. Gral. Flores 2124, 11800, Montevideo, Uruguay
[d] Laboratorio de Bioactividad y Nanotecnología de Alimentos, Departamento de Ciencia y Tecnología de Alimentos, Facultad de Química, Universidad de la República, Av. Gral. Flores 2124, 11800, Montevideo, Uruguay
[e] Department of Food Science, Faculty of Science, University of Copenhagen, Rolighedsvej 26, DK-1958, Frederiksberg, Denmark
[f] Advanced Bioimaging Unit, Institut Pasteur of Montevideo/Universidad de la República, Mataojo 2020, 11400, Montevideo, Uruguay

ARTICLE INFO

Article history:
Received 11 December 2023
Received in revised form
10 April 2024
Accepted 12 April 2024
Available online 20 April 2024

ABSTRACT

Wet-mixing processes can be tuned to reduce energy consumption, although impacts on quality and stability should be addressed. This work evaluated the effect of wet-mix processing (total solids, TS: 50 or 60%; heat treatment: 75 or 100 °C × 18 s) and storage conditions (open package: 25 °C, 58% RH, 4 weeks; closed package: 25 °C, multilayer bag, 12 weeks) on the physicochemical stability and digestibility of infant formulas. Processing significantly influenced the physicochemical characteristics of the powders, with TS exerting a stronger impact than heat treatment. Powders produced from 60% TS wet mixes presented the fastest water sorption, which accelerated lactose crystallisation and fat liberation. Formulas in closed packages were stable for 12 weeks. While lactose crystallised before week 2 in open-package storage, inducing major physical changes, only limited effects were observed on digestibility. These findings provide valuable insights to ensure consistent quality during shelf-life of infant formula.

1. Introduction

Infant milk formulas (IMF) are commonly presented in powder form produced by wet mixing. The production process includes the dispersion of the ingredients followed by heat treatment, homogenisation, concentration, and spray drying (Blanchard, Zhu, & Schuck, 2013). Although powders produced by wet-mix processing usually have superior quality (higher uniformity, better rehydration) compared to powders produced by dry-blending, it is also an extremely energy-intensive process (Montagne, Van Dael, Skanderby, & Hugelshofer, 2009). Therefore, research is currently focusing on developing new processes and technologies to reduce energy consumption associated with the production of such products (Patil, Tanguy, Floch-Fouéré, Jeantet, & Murphy, 2021).

A previous study showed that increasing the total solids (TS) content in the wet mix from 50 to 60% (w/w) while reducing the heat treatment temperature from 100 to 75 °C, decreased the energy consumption by 59% (Rodríguez Arzuaga et al., 2021a). However, such variations in the production process also had a strong impact on the physicochemical properties of the IMFs. Powders produced from wet mixes with higher TS had larger particle sizes and bulk densities and were less cohesive (Rodríguez Arzuaga et al., 2021b), and powders produced from wet mixes heat treated at 100 °C had a much higher degree of whey protein denaturation than those heat treated at 75 °C (Rodríguez Arzuaga et al., 2021a). It was also shown that the combination of TS level and heat treatment conditions of the wet mix significantly impacted the emulsion stability of the reconstituted powders (Rodríguez Arzuaga, Abraham, Ahrné, Pérez Montes, & Añón, 2022).

IMFs are usually packed in cans and are recommended to be consumed within 1 month after opening. During this month, the cans can be stored in high relative humidity environments, such as

* Corresponding author.
E-mail address: marodrig@latitud.org.uy (M. Rodríguez Arzuaga).

https://doi.org/10.1016/j.idairyj.2024.105968
0958-6946/

the kitchen, and opened several times a day, making the powder prone to moisture uptake. The high concentration of amorphous lactose is a challenging aspect of IMF stability during storage. If the moisture content of the powder increases, the lactose crystallisation accelerates, inducing the releasing of free fat and powder caking (Tham, Wang, Yeoh, & Zhou, 2016; Tham, Xu, Yeoh, & Zhou, 2017a). The effects of different factors related to the chemical composition of infant formulas, such as protein and lipid concentration, lactose/maltodextrin ratio or degree of whey protein hydrolysis, on their storage stability have been reported (Cheng et al., 2017, 2019; Masum, Chandrapala, Huppertz, Adhikari, & Zisu, 2020a; Saxena, Adhikari, Brkljaca, Huppertz, & Chandrapala, 2020; Saxena et al., 2021). Moreover, Masum, Chandrapala, Huppertz, Adhikari, and Zisu (2020b) stored powder infant formulas obtained by varying the air temperatures during spray drying and concluded that the powders spray dried at an outlet air temperature of 100 °C presented higher storage stability than powders dried at lower outlet air temperatures (80–90 °C), due to its lower initial moisture content. However, although varying pre-spray drying wet-mix processing parameters, such as wet mix TS and heat treatment, has a significant impact on the physicochemical characteristics of infant formula powders, as discussed before, their effects on the storage stability have not been published.

Previous works have demonstrated that the modifications of protein structures as a result of IMF processing may impact its digestibility (Bavaro et al., 2021; Halabi, Croguennec, Bouhallab, Dupont, & Deglaire, 2020). Therefore, and considering the crucial nutritional relevance of IMFs, that are designed to satisfy by themselves the nutritional requirements of infants under the age of 6 months (Codex Alimentarius, 2007), the effects of processing and storage on the digestibility of IMFs must be assessed. Hence, the current study was designed with the aim to investigate the impacts of the wet-mix processing conditions (TS and heat treatment temperature) and of the storage conditions (simulating open and closed package) on the physical stability and digestibility of IMF powders.

2. Materials and methods

2.1. Materials

The ingredients used for the infant milk formula (IMF) preparation were low-heat skim milk powder (Bützower Dauermilchwerk), whey protein isolate (Lacprodan®, Arla Foods Ingredients), lactose (Variolac 992, Arla Foods Ingredients), sunflower oil, galacto-oligosaccharides (GOS, Promovita®, Dairy Crest Limited) and fructo-oligosaccharides (FOS, Beneo Orafiti P95).

Model IMFs were produced by the wet-mix approach, at a pilot scale (batch = 15 kg), as detailed earlier (Rodríguez Arzuaga et al., 2021a). Two processing conditions: TS in the wet mix (50 or 60% w/w) and heat treatment (75 or 100 °C × 18 s) were varied to obtain four model IMFs: 50%-75 °C, 50%-100 °C, 60%-75 °C and 60%-100 °C. The IMFs were formulated according to the European infant formula regulations (European Commission, 2016), with a 60:40 whey protein:casein ratio. The average composition of the obtained powders was: protein (N × 6.25) = 11.3 ± 0.3 g/100 g, fat = 27.5 ± 1.7 g/100 g, lactose = 54.8 ± 2.3 g/100 g, GOS + FOS = 4.0 ± 0.8 g/100 g, and ash = 1.7 ± 0.1 g/100 g.

2.2. Storage conditions

All four IMF powder samples were stored under two different environmental conditions, simulating storage in open and closed packages. The open package storage conditions selected were: 58% RH and 25 °C. To achieve such conditions, each powder sample was fractionated in several 5-g subsamples, forming a thin layer in Petri dishes (diameter: 5.5 cm, height: 1.5 cm). Half of the Petri dishes from each IMF sample were randomly selected and placed in a vacuum tight desiccator containing a saturated solution of NaBr (58% RH at 25 °C). The remaining dishes were placed in another desiccator, containing the same volume of the NaBr solution. Both desiccators were stored in a temperature-controlled chamber at 24.3 ± 1.0 °C, for four weeks. Every week, five Petri dishes of each IMF sample were removed from both desiccators for analysis.

For the closed package storage, two subsamples (20 g) of each IMF powder (8 in total) were weighed and packed in sealed film laminate metal layered bags (Statshield® moisture barrier bag, DESCO, USA) and stored in the temperature-controlled chamber at 24.3 ± 1.0 °C. All bags were removed from the chamber and open for analysis after 12 weeks of storage.

2.3. Water activity and moisture content

Water activity (a_w) and moisture content of the IMF powders were analysed in duplicate. Water activity was measured at 25 °C using an Aqualab 47EV (Decagon Devices Inc., CA, USA) calibrated with 13.41 M LiCl. Moisture content was determined according to GEA Niro method No. A1a (GEA Niro, 2006).

2.4. Glass transition and crystallisation

Glass transition temperature (Tg) and crystallisation temperature (Tcr), of the time 0 and stored IMF powders were determined in triplicate, using a differential scanning calorimeter (Q2000 DSC, TA Instruments, DE, USA) calibrated with Indium. Samples (8–10 mg) were scanned in hermetically sealed aluminium pans, using an empty pan as reference. Samples were first heated from 0 to 100 °C at a rate of 10 °C min^{-1}, followed by cooling to 0 °C at 5 °C min^{-1}, and then heated until 160 °C at 5 °C min^{-1}. Onset Tg and Tcr were determined in the final heating step.

Crystallinity of the IMF powders was also evaluated by X-ray diffraction (XRD). Samples ~100 mg in weight were mounted on a glass sample holder and placed in the centre of the goniometer of a Rigaku ULTIMA IV powder diffractometer operating in Bragg–Brentano θ–θ geometry using Cu$K\alpha$ radiation tube source (λ = 1.5418 Å) and a curved-Ge monochromated NaI scintillator detector both placed at 285 mm of the rotation axis. Diffraction scans were obtained with the source at 40 kV/30 mA power scanning from 5 to 60° 2θ with a step of 0.04° for 10 s to confirm crystallinity. Samples (~200 mg determined exactly) were mixed with ~10 mg of crystalline valine (determined exactly) and ground together until mixed to obtain a ~5% w/w valine/formula for quantitative phase analysis. Diffraction data was collected over a 5–80° in 2θ and 0.02° step for 15 s/step and analysed using the Rietveld method (Rietveld, 1969) implemented in GSAS-II software (Toby & Von Dreele, 2013).

2.5. Surface free fat

Surface free fat (SFF) was quantified in the powders throughout storage, according to the method proposed by Kim, Chen, and Pearce (2009) with some modifications. Briefly, 1 g of powder was accurately weighted on a MN 614 filter paper (Macherey-Nagel, Germany), equivalent to Whatman No. 4, and washed with 4 × 50 mL 30–65° petroleum ether portions. The filtrate containing the extracted surface free fat was allowed to evaporate until constant weight. Experiments were performed in triplicate. SFF content was expressed per gram of total fat and calculated according to Equation (1).

$$SFF\left(\frac{g}{100\ g\ total\ fat}\right) = \frac{EF \times 100}{Powder \times \frac{TFC}{100}} \quad (1)$$

where *EF* (extracted fat) represents the weight of the dried filtrate (g), *Powder* represents the weight of the initial powder sample (g) and *TFC* (g/100 g) represents the total fat content of the powder sample in wet basis.

2.6. Confocal laser scanning microscopy

Surface free fat of the IMFs was also qualitatively assessed with confocal laser scanning microscopy (CLSM), using a confocal Zeiss LSM 800 microscope (Oberkochen, Germany) with a Zeiss 63× Plan-Apochromat NA 1.4 oil immersion objective lens. The powder samples were placed on a slide and 10 μL of a mixture (1:10) of Nile Red (0.10 g L^{-1} in propylene glycol) and Fast Green (0.1 g L^{-1} in dimethyl sulfoxide) was deposited on the powder samples, to label the fat and protein components of the powders, respectively. The powders with the mixture were let stand for 1 min before covering the samples with a cover slip. The Fast Green and Red Nile fluorescence were visualized with an Ar laser (excitation = 488 nm, emission = 400–600 nm) and a He–Ne laser (excitation = 640 nm, emission = 656–700 nm), respectively. To obtain panoramic images, the tile scan tool of the Zen blue software version 3.5 was used. Using this plugin, tile images of 25 tiles were created. The final image was 4711 × 4710 pixels, which is equivalent to 666.51 × 666.37 μm. The pixel size in all cases was 0.141 μm.

2.7. Scanning electron microscopy

Surface morphology of the powder particles was evaluated using scanning electron microscopy (SEM). The powder samples were coated with gold for 120 s at 30 mA and analysed in a JSM-5900LC scanning electron microscope (JEOL USA Inc., MA, USA).

2.8. *Static* in vitro *gastro-intestinal digestion*

In vitro gastric and intestinal digestion of the IMF samples before (time 0) and at the end of open package-like storage (week 4) and closed package-like storage (week 12) was carried out using the method proposed by Ménard et al. (2018). The authors excluded the oral phase, as the time of residence of the reconstituted infant formula in the mouth is short. The powders were rehydrated overnight on a 1.4% (w/w) protein basis before being subjected to both gastric and intestinal digestion. For the gastric digestion, the reconstituted IMF was mixed with simulated gastric fluid (SGF, 94 mM NaCl, 13 mM KCl, pH 5.3) in a meal: SGF ratio of 63:37 and the pH was adjusted to 5.3. Samples taken at this point were recorded as G0 for analysis. Porcine pepsin (268 U mL^{-1}, Sigma Aldrich) and lipase from bovine pancreas (19 U mL^{-1}, Sigma Aldrich) were added to the IMF + SGF mixture and the pH was readjusted to 5.3 if necessary. Digestion was carried out in a shaking (50 rpm) water bath maintained at 37 °C. After 60 min, the pH of the tubes was adjusted to 7.0 to stop the enzyme action, and 10-mL samples were taken and recorded as G60 for further analysis. For intestinal digestion, simulated intestinal fluid (SIF, 164 mM NaCl, 10 mM KCl, 85 mM $NaHCO_3$, pH 6.6), and appropriate volumes of bile salts solution (0.05 mmol mL^{-1} Sigma Aldrich), $CaCl_2$ (0.018 mmol mL^{-1}) and porcine pancreatin (Sigma Aldrich), preheated at 37 °C, to reach in each tube: meal: SGF + SIF ratio of 39:61, lipase activity from pancreatin of 90 U mL^{-1}, bile salts concentration of 3 mM in the total volume and $CaCl_2$ concentration of 3 mM in the SIF volume. If necessary, pH was adjusted to 6.6, before incubation in a water bath (50 rpm shaking, 37 °C) for further 60 min. After digestion, tubes were identified as I60 and handled according to posterior analysis. pH was monitored during gastric and intestinal digestion. Gastric and intestinal digestions were conducted in duplicate for each IMF sample and blanks (substituting the IMF sample by water) were run in parallel.

2.8.1. Protein digestion patterns

SDS-PAGE of the *in vitro* digests was carried out under reducing conditions. The G0, G60 and I60 (immediately after intestinal incubation and without further treatment) were mixed with a 1.5 mg mL^{-1} SDS solution and 2-mercaptoethanol in the following ratios: 4.5:38.5:1 for G0: SDS:2-mercaptoethanol, 5:38:1 for G60:SDS:2-mercaptoethanol and 8:38:1 for I60:SDS:2-mercaptoethanol, and frozen until analysis. On the day of the analyses, the mixed samples were thawed and mixed with a reducing buffer in a 4:1 mix: buffer ratio and heated in a boiling water bath for 5 min to ensure the unfolding of proteins. A 10–180 kDa molecular weight ladder (#26616, ThermoScientific, USA) was also run. The analysis was conducted as described previously (Rodríguez Arzuaga et al., 2022).

2.8.2. Degree of proteolysis

The degree of protein hydrolysis was determined in the G0 (before gastric enzymes addition), G60 (after stopping gastric enzymes action by adjusting pH to 7.0) and I60 digesta (after inactivating intestinal enzyme by incubation in a water bath at 85 °C for 10 min). Oil phase was carefully removed from the samples after centrifugation (Thermo Scientific Sorvall™ ST 8R, MA, USA) at 4000×*g* and 20 °C for 20 min, and the aqueous supernatants were freeze-dried (BIOBASE BK-FD10S benchtop freeze dryer, Shandong, China) and frozen until analysis. The degree of hydrolysis was determined by quantification of the free amino groups reacting with *o*-phthaldialdehyde (OPA), as described by Nielsen, Petersen, and Dambmann (2001). A calibration curve was prepared using L-leucine (Merck) as standard. For the analysis, the freeze-dried samples were reconstituted in 1 mL of 0.1 M borate 0.1% SDS buffer. Standard or an appropriate sample dilution (200 μL) were added to the OPA reagent, and the absorbance was measured exactly 2 min later, at 340 nm in a Mettler Toledo UV5 spectrophotometer (OH, USA). Analyses were carried out in triplicate.

2.8.3. Degree of lipolysis

The degree of lipolysis was quantified through analysis of the percentage of fatty acids released (FFA) during digestion, by AOAC method 947.05 (AOAC International, 2016), on the samples before digestion (G0) and after gastro-intestinal digestion (I60). The latter were frozen immediately after simulated intestinal digestion without further treatment and until analysis. G0 and I60 were titrated with 0.1 N NaOH until pH 8.4. Each digest was analysed in duplicate and the FFA content in G0 and I60 was expressed as g of oleic acid in 100 mL of reconstituted IMF. The dilutions occurring during digestion were considered for the calculations and the oleic acid was chosen because it is the main fatty acid in sunflower oil, the only source of fat in the model formulas. The results were expressed as FFA in I60 − FFA in G0, to only account for the FFA liberated during the simulated digestion process.

2.9. Statistical analysis

Analysis of variance (ANOVA) were performed to determine significant differences ($\alpha = 0.05$) between IMFs (50%-75 °C, 50%-100 °C, 60%-75 °C, 60%-75 °C) for a given storage time and condition, and between times during open package conditions. Post-hoc Tukey's tests were performed at a level of confidence of 95%.

Student t-tests were performed to determine significant differences ($\alpha = 0.05$) between time 0 and 12 weeks of storage under closed package conditions.

All statistical analyses were performed by means of InfoStat software version 2020.

3. Results and discussion

3.1. Water sorption, glass transition and crystallisation

At time 0, the a_w and moisture content of the IMFs varied between 0.11–0.15 and 0.8–1.2 g/100 g, respectively (Fig. 1), and there were no significant differences ($p > 0.05$) among IMFs' glass transition (Tg) or crystallisation (Tcr) temperatures. All Tg values were much higher than the powder temperature (25 °C), indicating that all powders were in the glassy amorphous region (Table 1).

Under open package storage conditions, a_w increased until week 2 (Fig. 1A), while the moisture content showed an increasing trend until week 1, followed by a reduction at week 2 (Fig. 1B). As expected, as the moisture in the formulas increased during the first week of storage, an important reduction of Tg and Tcr was obtained for all samples (Table 1), since the water in the samples plasticizes and induces the mobility of the lactose molecules. At week 1, the Tg of the four formulas was below the storage temperature ($Tg < 25$ °C), indicating that all samples were already at the rubbery amorphous region. Moreover, 60% TS formulas presented significantly ($p < 0.05$) lower Tg and Tcr than 50% TS formulas. These differences are explained by the higher a_w values obtained for 60%-75 °C and 60%-100 °C, at this sampling time (Fig. 1A). The onset Tcr values obtained at week 1 decreased as follows: 50%-75 °C > 50%-100 °C > 60%-75 °C > 60%-100 °C (Table 1). Therefore, for a given a_w ($a_w \approx 0.44$ for 50% TS formulas and $a_w \approx 0.48$ for 60% TS formulas), the IMFs pasteurised at 75 °C had higher Tcr than the IMFs pasteurised at 100 °C, which can be associated with a higher storage stability. Jouppila, Kansikas, and Roos (1997) demonstrated that the rate of lactose crystallisation increases with RH, moisture content and with the difference between the powder temperature (25 °C in the present study) and Tg (T − Tg). At week 1, T − Tg for 50%-100 °C (8.7 °C) was larger than for 50%-75 °C (5.9 °C), explaining the higher crystallisation rate, given by the lower Tcr value. On the other hand, the difference between the Tcr obtained for 60%-75 °C and 60%-100 °C, is not explained by T − Tg, since there were no significant differences between their Tg values. By week 1, the moisture content in 60%-100 °C (7.7 ± 0.1 g/100 g) was significantly higher ($p < 0.05$) than in 60%-75 °C (7.2 ± 0.1 g/100 g) (Fig. 1), accounting for the Tcr difference between the 60% TS formulas. From week 2 of storage in open package, no changes were detected in the heat flows during the DSC assays of the formulas, indicating that they were already completely crystallised, in agreement with the a_w and moisture content results (Fig. 1). Similarly, Cheng, Erichsen, Soerensen, Petersen, and Skibsted (2019) reported that the Tg of commercial infant formula was not detectable after two weeks of storage at $a_w = 0.53$ and 40 °C.

While at week 2, 60%-75 °C and 60%-100 °C had already reached equilibrium ($a_w = 0.58$), a_w of 50% TS samples was above ambient RH. These small differences between formulas produced from wet mixes with 50 or 60% TS, indicate a higher rate of water sorption of 60%-75 °C and 60%-100 °C formulas, possibly explained by morphological characteristics, which will be addressed later. Moreover, the decrease in water content accompanied by an increase of a_w between weeks 1 and 2 can be explained considering that crystalline lactose has a lower water capacity than amorphous lactose, hence water is liberated during crystallisation, decreasing the overall moisture content of the sample (Palzer, 2010). The results suggest that crystallisation occurred in the four samples between weeks 1 and 2 (i.e., at a_w 0.43–0.61 for 50%-75 °C, 0.46–0.61 for 50%-100 °C and 0.48–0.57 for 60%-75 °C and 60%-100 °C), but probably a few days earlier in 60% TS samples, which led to earlier water liberation and reaching of equilibrium.

After 12 weeks of closed package storage, a significant ($p < 0.05$) increase in the moisture content was observed in all samples, probably due to the absorption of water present in the bag headspace, which led to a reduction in the Tg and Tcr values compared to time 0 (Table 1). However, Tg and Tcr were well above the storage temperature (Tg > 60 °C and Tcr > 128 °C) in the four IMFs, hence lactose was in amorphous state. Although no significant differences ($p > 0.05$) were found among the moisture contents of the formulas at week 12, 60% TS IMFs showed higher ($p = 0.0017$) a_w (0.27) than 50% TS IMFs ($a_w = 0.21$–0.22), in agreement with the fastest moisture sorption obtained for 60% TS IMFs during open package storage.

Lactose crystallisation is a complex process because it is a reducing sugar that can exist in two anomeric forms: α and β-

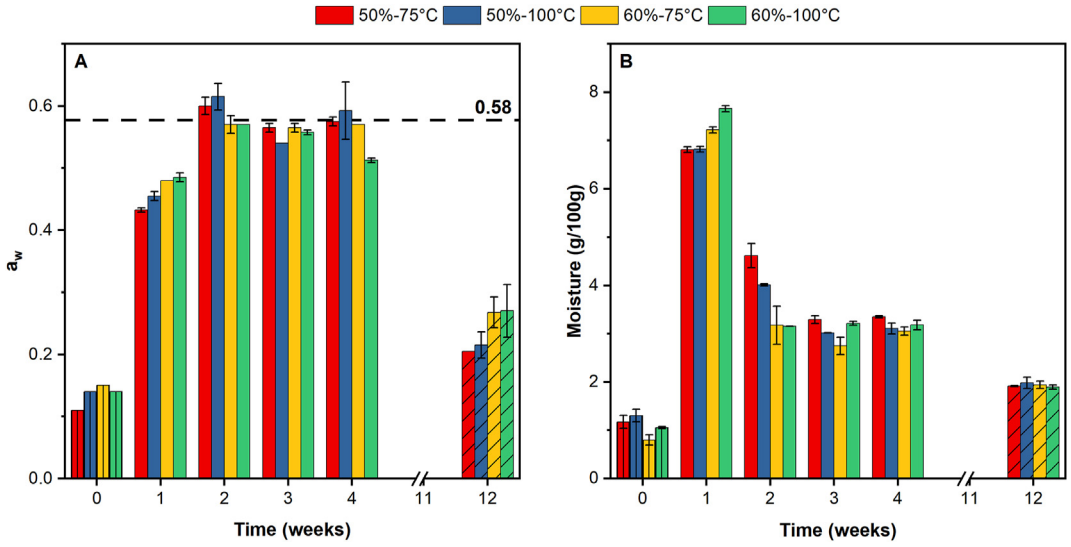

Fig. 1. Water activity (a_w, A) and moisture content (B) of the 50%-75 °C (red), 50%-100 °C (blue), 60%-75 °C (yellow) and 60%-100 °C (green) model infant milk formulas, before storage (bars with vertical lines), during storage under open package conditions (smooth bars) and after 12 weeks of storage under closed package conditions (bars with diagonal lines). Error bars indicate standard deviation (n = 4). Dashed line in A indicates ambient relative humidity during open package storage (58%).

Table 1
Onset glass transition (Tg) and crystallisation temperatures (Tcr) of the model infant formulas, before storage (Time 0), after 1 week under open package storage conditions (Week 1), and after 12 weeks under closed package storage conditions (Week 12).

IMF	Tg (°C)			Tcr (°C)		
	Time 0	Week 1	Week 12	Time 0	Week 1	Week 12
50%-75 °C	70.8 ± 1.9^{a}	19.1 ± 0.7^{c}	64.6 ± 1.1^{b}	135.1 ± 0.3^{a}	81.5 ± 0.8^{d}	134.7 ± 2.9^{b}
50%-100 °C	69.4 ± 1.5^{a}	16.3 ± 0.7^{b}	64.8 ± 1.6^{b}	134.2 ± 1.6^{a}	75.7 ± 1.2^{c}	131.9 ± 4.6^{ab}
60%-75 °C	71.4 ± 1.4^{a}	11.6 ± 0.9^{a}	60.9 ± 1.1^{a}	134.2 ± 0.7^{a}	69.1 ± 0.5^{b}	134.5 ± 2.4^{b}
60%-100 °C	71.3 ± 1.8^{a}	10.5 ± 1.3^{a}	62.3 ± 1.0^{a}	133.8 ± 0.6^{a}	62.7 ± 2.3^{a}	128.5 ± 1.0^{a}

Mean ± standard deviation (n = 6). Different letters between rows indicate significant differences ($p < 0.05$) between formulas, for each storage time.

lactose. Furthermore, amorphous lactose can crystallise into various crystalline forms (polymorphism), depending on the crystallisation conditions (Biliaderis, Lazaridou, Mavropoulos, & Barbayiannis, 2002; Haque & Roos, 2005). Therefore, the crystallisation of the powders was also evaluated by DRX. Fig. 2 shows the diffraction data for the IMFs during open package storage. Note that peaks in the lowest-lying diagrams (representing time 0) correspond to the mixture of the amorphous formula and the added valine internal standard. The peaks corresponding to L-valine in the range 5–35° are located at 2θ diffraction angles of 7.4°, 14.7°, 22.1° and 29.7° (Sangeetha, Mariappan, Madhurambal, & Mojumdar, 2015). At time 0, the four formulas were completely amorphous (the only diffraction peaks present are those corresponding to valine), and this was maintained after 1 week of storage in open package (Fig. 2). After 2 weeks, all four formulas showed crystallisation, confirming the DSC results (Table 1). No significant differences were observed between the diffraction data of the IMFs, at week 2. No significant differences were observed between the diffractograms obtained at weeks 2 and 4, in the position, intensity or shape of diffraction peaks, indicating that crystallisation did not progress and, therefore, the formulas were already completely crystallised by week 2. This result is also in line with the

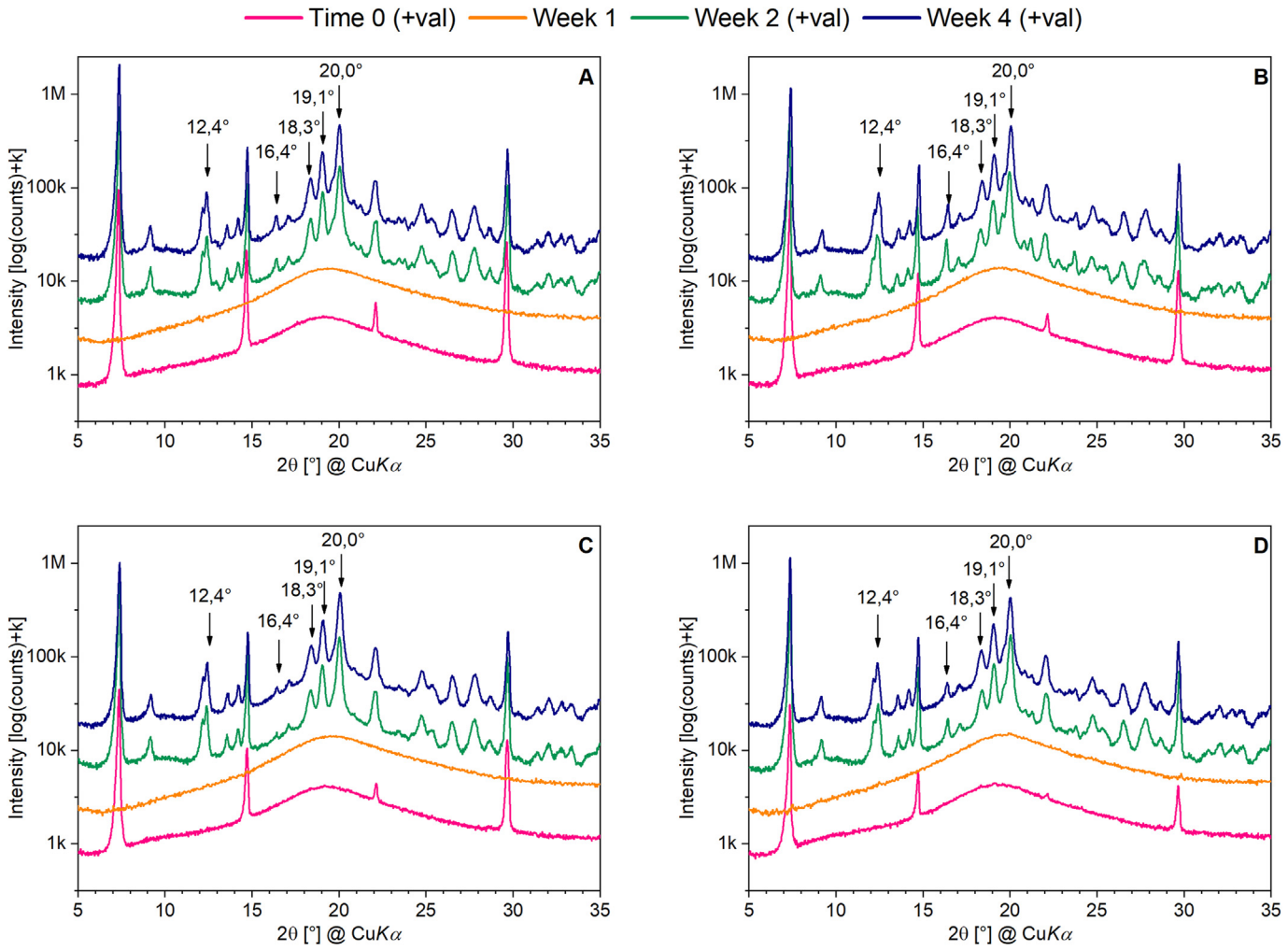

Fig. 2. X-ray diffraction data for 50%-75 °C (A), 50%-100 °C (B), 60%-75 °C (C) and 60%-100 °C (D) infant milk formulas, before storage (magenta), after 1 week (orange), 2 weeks (green) and 4 weeks (blue) of storage under open package conditions. The formulas at time 0 and weeks 2 and 4 were mixed with L-valine (+val) for crystalline-phase quantification. Arrows indicate peaks at characteristic diffraction angles (2θ).

thermograms obtained by DSC, in which no transition was obtained from the second week. Therefore, crystallisation occurred in the formulas at 25 °C and a_w = 0.43–0.49 (Fig. 1), coinciding with previous reports for products of similar composition (Haque & Roos, 2005; Tham et al., 2016).

The identification of the crystalline forms present from week 2 onwards was carried out based on bibliographic information. Crystals of α-lactose monohydrate were detected, which presents peaks at diffraction angles 2θ 12.4°, 16.4° and 20° (Drapier-Beche, Fanni, Parmentier, & Vilasi, 1997; Miao & Roos, 2005), in the four formulas stored for at least 2 weeks in open package (Fig. 2). Although, the peak with a maximum at 12.4° corresponds to two peaks with diffraction angles at 12.1 and 12.4°, in agreement with Nijdam, Ibach, Eichhorn, and Kind (2007). However, since peaks at 20° and 12.4° have also been reported for other crystalline forms (Biliaderis et al., 2002; Nijdam et al., 2007), the peak at 16.4° is used to establish the presence of α-lactose monohydrate.

The peaks at 19.1 and 20.0° have been attributed to the α-/β-lactose mixture in a 5:3 molar ratio (Biliaderis et al., 2002; Miao & Roos, 2005; Simpson, Parrish, & Nelson, 1982), and, according to Nijdam et al. (2007), the best peak to characterize the mixture in molar ratio α:β = 5:3 is found at a 2θ of ~18.2°, which was also detected in the four formulas (~18.3°). Despite multiple studies reporting the existence of a crystalline form of lactose with molar ratio α:β = 5:3 (Biliaderis et al., 2002; Fan & Roos, 2015; Saffari & Langrish, 2014), there are no reports of powder diffraction of a pure phase or of the crystalline structure of solids with such molar ratio in the databases of the International Center for Diffraction Data (ICDD, 2013) or in the Cambridge Structural Database (CSD, 2021) (Groom, Bruno, Lightfoot, & Ward, 2016). This suggests that the form of lactose with ratio α:β = 5:3 does not really exist, being α-β-lactose or a mixture of this phase with other anhydrous forms reported for α-lactose. Anhydrous β-lactose presents peaks at 2θ = 10.4–10.5° and 20.9–21.0°, with the peak at ~10.4° being the one that best characterises it, as it is unique for this form (Kirk, Dann, & Blatchford, 2007), therefore, the absence of this peak indicated that the formulas did not present crystals of anhydrous β-lactose. Similarly, the α-/β-lactose mixture in a 4:1 molar ratio was not detected, for which peaks have been reported at 12.8° (Jouppila, Kansikas, & Roos, 1998) and 19.5° (Miao & Roos, 2005).

Despite the apparent lack of consensus on the existence of crystals composed of α- and β-anhydrous lactose (Hourigan, Lifran, Vu, Listiohadi, & Sleigh, 2013), we attempted to fit the powder diffraction datasets of the four fully crystallized IMFs using crystal structures corresponding to α-/β-D-lactose (Guiry, Coles, Moynihan, & Lawrence, 2008) and α-lactose monohydrate (Fries, Rao, & Sundaralingam, 1971) obtaining a very acceptable fit (Fig. 1.S) and the total calculated lactose weight percentage equal to the preparation composition within experimental uncertainty.

After 12 weeks of storage in closed package, the four formulas were completely amorphous (Fig. 2.S), in agreement with the DSC results (Table 1). The diagrams obtained at time 0 presented only the peaks corresponding to the internal standard L-valine, with which each sample was mixed, while the diagrams obtained at 12 weeks did not present peaks.

3.2. Surface free fat

Initially (time 0), there were no significant differences ($p > 0.05$) between the surface free fat (SFF) contents of the formulas, which ranged 0.65–1.10% of total fat (Fig. 3). SFF increased in the four IMFs during open package storage. After 1 week, 60%-75 °C presented the greatest SFF content (8.1 ± 0.6%), followed by 50%-100 °C (6.3 ± 0.8%), while 50%-75 °C and 60%-100 °C presented the lowest SFF contents (3.1%). The emulsion properties of the reconstituted

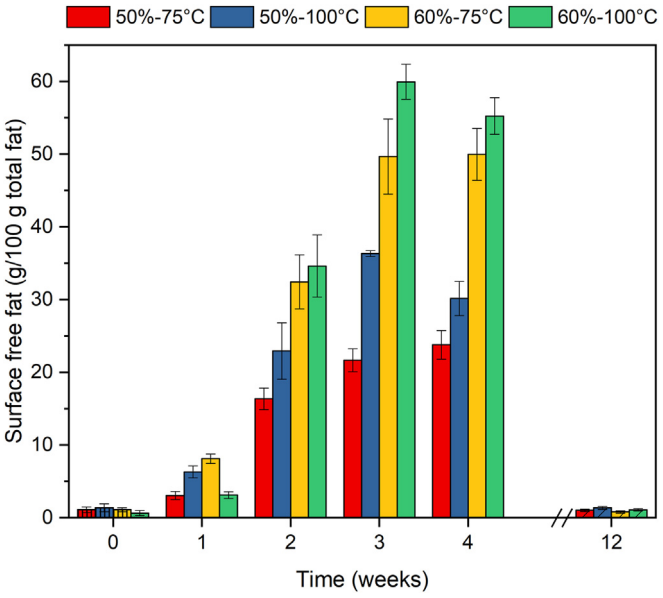

Fig. 3. Surface free fat of the 50%-75 °C (red), 50%-100 °C (blue), 60%-75 °C (yellow) and 60%-100 °C (green) model infant milk formulas, before storage (bars with vertical lines), during storage under open package conditions (smooth bars) and after 12 weeks of storage under closed package conditions (bars with diagonal lines). Error bars indicate standard deviation (n = 3).

IMFs were evaluated in a previous study, where 60%-75 °C was found to be the least stable emulsion (with flocculated oil droplets), while 50%-100 °C presented the largest individual oil droplet diameters (Rodríguez Arzuaga et al., 2022). Therefore, during the first week of storage under open package conditions, the migration of free fat to the surface appeared to be related with the emulsions' stability.

A sharp increase in SFF was observed between weeks 1 and 2 of storage (Fig. 3), in parallel to the lactose crystallisation, as discussed earlier. The increase in SFF in dairy powders as a result of lactose crystallisation has been reported (Masum et al., 2020b; McCarthy et al., 2013; Vega, Douglas Goff, & Roos, 2007). The formation of lactose crystals can damage the oil droplets, releasing the fat, and promoting its migration to the particles' surface (Vignolles, Jeantet, Lopez, & Schuck, 2007). In all IMFs containing crystallised lactose (weeks 2, 3 and 4), SFF was significantly higher ($p < 0.05$) in 60%-75 °C and 60%-100 °C than in powders produced from 50% TS wet mixes. After 4 weeks of storage, 24–30% of the total fat in 50%-75 °C and 50%-100 °C corresponded to free fat, while SFF in 60%-75 °C and 60%-100 °C reached 50–55% (Fig. 3). The a_w and moisture content results suggested that water sorption occurred faster in 60% TS than in 50% TS IMF samples (Fig. 1), which accelerated the Tg reduction and lactose crystallisation (Table 1). Similarly, Masum et al. (2020a) found a correlation between SFF and Tg of IMF powders: formulas with lower Tg presented larger SFF contents during storage.

Under closed-package storage conditions, none of the formulas showed a significant increase in SFF, after 12 weeks (Fig. 3). All four IMF samples were completely amorphous at week 12, reinforcing the hypothesis that the main increase in the SFF during storage is due to the lactose crystallisation.

Fig. 4 shows the confocal laser scanning microscopy (CLSM) micrographs of the IMF powders before storage and after open and closed package storage, where the protein networks and oil droplets were labelled. At time 0 (Fig. 4A), 50%-100 °C and 60%-100 °C presented large protein aggregates, induced by the high heat treatment temperature (100 °C) applied during processing. By the

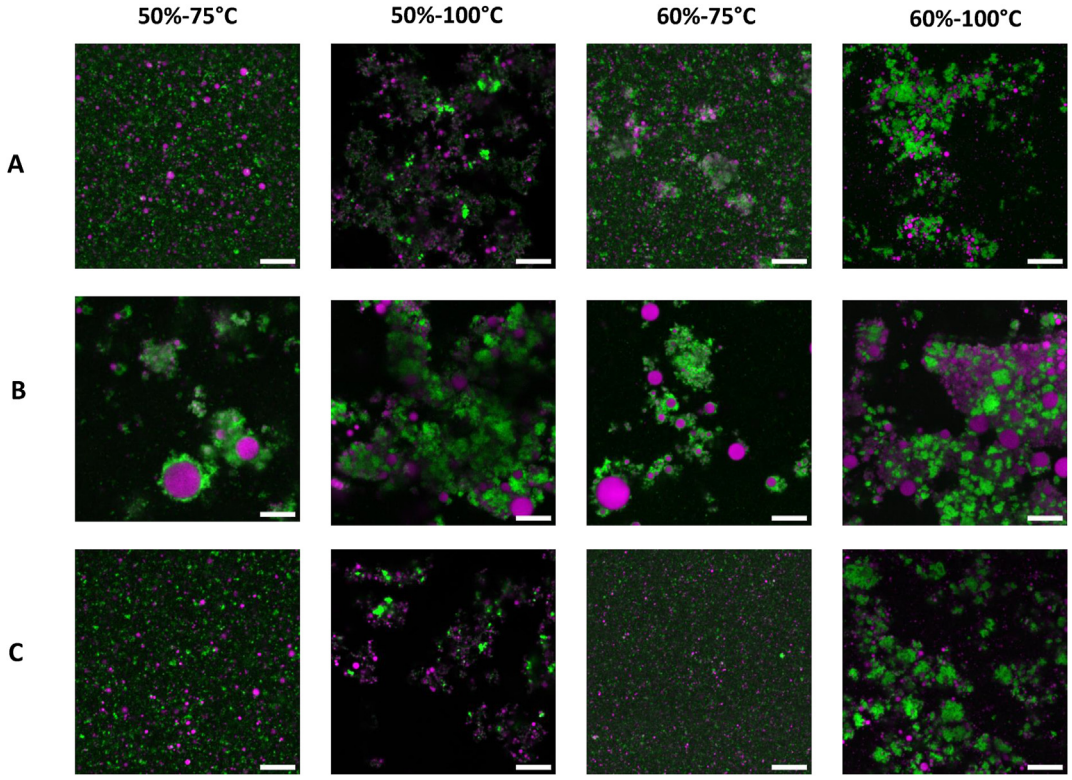

Fig. 4. Confocal laser scanning microscopy (CLSM) micrographs of the model infant milk formulas, before storage (time 0, A), after 4 weeks of storage under open package conditions (B) and after 12 weeks of storage under closed package conditions (C). The protein networks were stained with Fast Green and appear in green colour, the fat networks were labelled with Nile Red and appear in magenta colour. Scale bars represent 20 μm.

end of the open package storage, all four samples showed a significant increase in the oil droplet size (Fig. 4B). This result indicates the flocculation or coalescence of small oil droplets, induced after their liberation from the protein network, which led to the increased SFF content obtained at week 4 (Fig. 3). Similarly, Tham et al. (2017a) and Tham, Yeoh, and Zhou (2017b) observed an increase of the fat globules size as a result of the agglomeration of small fat globules, in aged commercial infant formulas powders, which also resulted in a higher SFF content. On the other hand, and in line with the SFF results, no noticeable changes were observed after 12 weeks of closed package storage (Fig. 4C).

3.3. Scanning electron microscopy

Fig. 5 shows the scanning electron microscopy (SEM) images for the stored IMF powders. Initially (Fig. 5A), all IMF powders presented individual spherical particles. The surface of the particles was mainly smooth and the bulk powders presented a range of particle sizes, with the mean diameter increasing in the following order: 50%-75 °C < 50%-100 °C < 60%-75 °C < 60%-100 °C. The observed differences in the particle sizes is in agreement with the laser diffraction results reported and explained earlier as a consequence of the increase in the viscosity of the wet mixes obtained when increasing both the TS and the heat treatment temperature (Rodríguez Arzuaga et al., 2021b). Broken particles were detected in the powders produced from 60% TS wet mixes, which were the powders with the largest particle size, exposing the porous interior of the particles. This result is aligned with previous studies reporting that smaller sized particles are more resistant to breakage (Han, Fitzpatrick, Cronin, Maidannyk, & Miao, 2022; Han, Fitzpatrick, Cronin, Maidannyk, & Miao, 2021c; Han, Fitzpatrick, Cronin, & Miao, 2021b). The type of breakage observed at time 0, in 60%-75 °C and 60%-100 °C, seemingly corresponds to surface breakage (abrasion or chipping), which is associated with limited particle damage and low load levels on the particles (Han et al., 2021c). Breakage is likely to occur during post spray-drying processes, such as agglomeration in fluidized bed, transportation, packaging (Han, Fitzpatrick, Cronin, & Miao, 2021a). Since such processes were not applied during the production of the samples, breakage probably occurred during the handling of the powders. Breakage has shown to increase the specific surface area of the powders, which explains the faster water sorption obtained for 60%-75 °C and 60%-100 °C compared to 50%-75 °C and 50%-100 °C.

After 1 week of open package storage (Fig. 5B), it was still possible to distinguish smooth spherical particles, but the presence of liquid bridges connecting the particles was evident in the four samples. After two weeks, the particles' surfaces changed from smooth to rough and irregular and the individuality of the particles was lost. This change could be explained by the lactose crystallisation. Although no sharp lactose crystals were observed, such crystals were probably present and located under a layer of fat that was covering the surface, as explained by Murrieta-Pazos et al. (2011). At week 4, all IMFs were caked, and it was not possible to distinguish individual powder particles. Furthermore, the presence of smooth rounded bumps was noted in the four formulas at week 4, but also in 60%-75 °C and 60%-100 °C, at week 2. The shape of the bumps suggests that they were oil droplets, that were released from the matrix.

The surface microstructure of the formulas presented almost no variations after 12 weeks of closed package storage (Fig. 5C). All four IMFs still had individual spherical-shaped particles with relatively smooth surfaces, and no lumps were detected. The observed microstructure agrees with the previously presented results, which showed that after the closed package storage, the

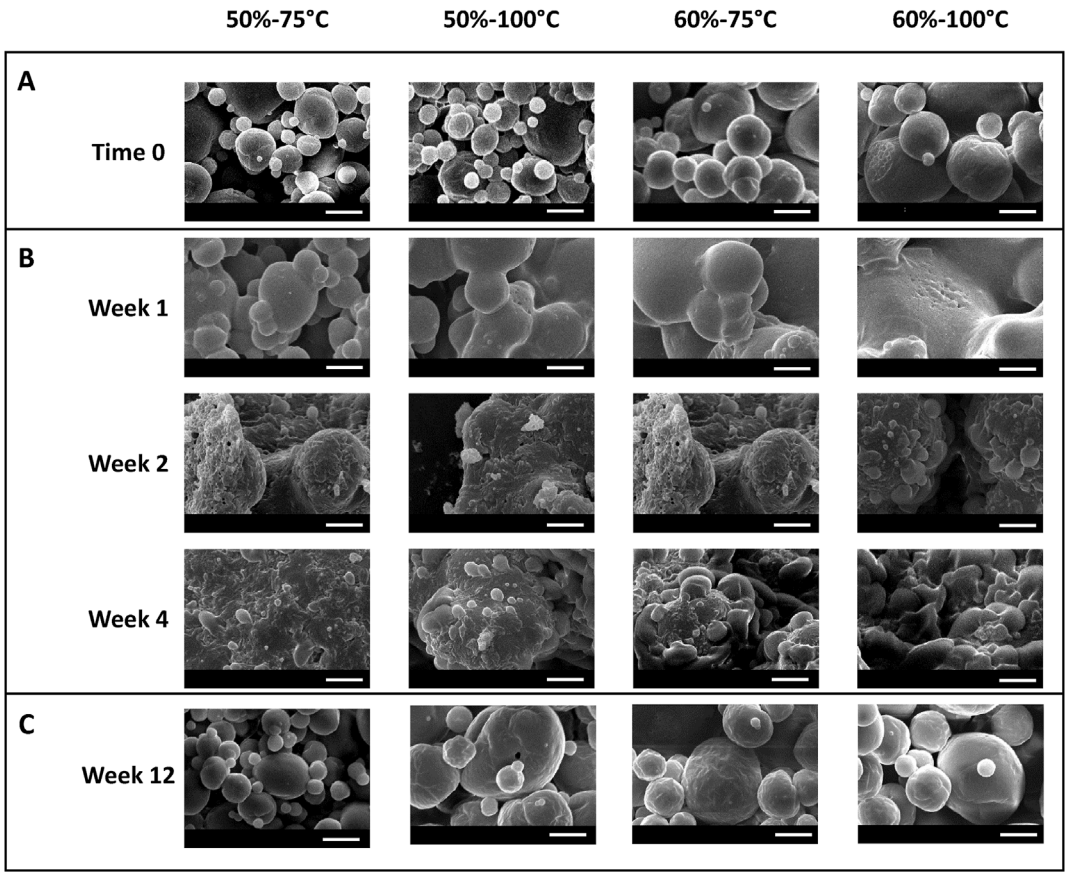

Fig. 5. Scanning electron micrographs of the model infant milk formulas, before storage (time 0, A), after 1, 2 and 4 weeks of storage under open package conditions (B) and after 12 weeks of storage under closed package conditions (C), at 2500× magnification. Scale bars represent 10 μm.

formulas had low a_w (0.20–0.27, Fig. 1), with no significant SFF increase (Fig. 3), and that the lactose remained in an amorphous glassy state (Table 1, Fig. 2). On the other hand, the 60% TS formulas showed more wrinkled surface after 12 weeks, indicating certain level of water sorption, in agreement with the a_w results (Fig. 1).

3.4. *Static* in vitro *gastro-intestinal digestion*

Finally, the IMF samples obtained under varying processing conditions and storage conditions, were subjected to a static *in vitro* gastro-intestinal digestion procedure.

3.4.1. *Degree of proteolysis*

Fig. 6A shows the degree of proteolysis achieved during *in vitro* digestion of the formulas and Fig. 6B shows the SDS-PAGE profile of the digested formulas. The protein profile of the whey dominant IMFs comprised 40% caseins and 60% whey proteins, being β-lactoglobulin and α-lactalbumin the most abundant. Before addition of the gastric enzymes (G0), a band corresponding to β-lactoglobulin (~18 kDa) and α-lactalbumin (~14 kDa), two bands between 34 and 43 kDa, corresponding to αs- and β-casein, and a band between 26 and 34 kDa, corresponding to κ-casein, were detected at the three storage points (Fig. 6B).

In the first stage (gastric), proteolysis occurred by action of pepsin enzyme, at 37 °C and pH = 5.3 for 60 min. After this phase (G60), the formulas displayed degree of hydrolysis in the range 21–44% (Fig. 6A), and an important reduction in the intensity of bands was observed in all the formulas, together with the appearance of bands in the lower area of the gel, corresponding to low molecular weight peptides (Fig. 6B). Then, during the intestinal stage, carried out at 37 °C and pH = 6.6 for 60 min, protein hydrolysis continued, and, at completion of digestion (I60, 60 min gastric + 60 min intestinal), formulas averaged 42–75% protein hydrolysis. These percentages are aligned with previously published values for infant formulas (Halabi et al., 2020; Li et al., 2020).

Storage conditions did not make a significant impact on the degree of proteolysis during the digestion of the model formulas (Fig. 6A). Further, no preferential protein hydrolysis was detected during simulated digestion, as a result of processing or storage condition (Fig. 6B). However, processing conditions made a significant impact ($p < 0.05$) on the degree of proteolysis. For all storage conditions (time 0, 4 weeks in open-package and 12 weeks in closed-package), the highest proteolysis was obtained for 60%-75 °C, and that difference was more pronounced at I60 than at G60. 60%-75 °C was submitted to the mildest heat treatment (75 °C × 18 s) which induced a low degree of whey protein denaturation and aggregation (8%), as reported elsewhere (Rodríguez Arzuaga et al., 2021a). Although no significant differences were found between the denaturation/aggregation levels in 60%-75 °C and 50%-75 °C, the latter showed significantly lower ($p < 0.05$) proteolysis after digestion, for the three storage conditions (Fig. 6A). Previous work examined the emulsion stability of the four IMF powders and found that reconstituted 60%-75 °C was flocculated and less stable, and had the highest level of β-lactoglobulin adsorbed at the oil-water interface (Rodríguez Arzuaga et al., 2022). The adsorption of β-lactoglobulin at hydrophobic interfaces enhances its susceptibility to pepsin proteolysis, compared to soluble β-lactoglobulin (Bourlieu et al., 2015; Macierzanka, Sancho, Mills, Rigby, & MacKie, 2009). Therefore, the processing conditions (combination of TS level and heat treatment) impacted the

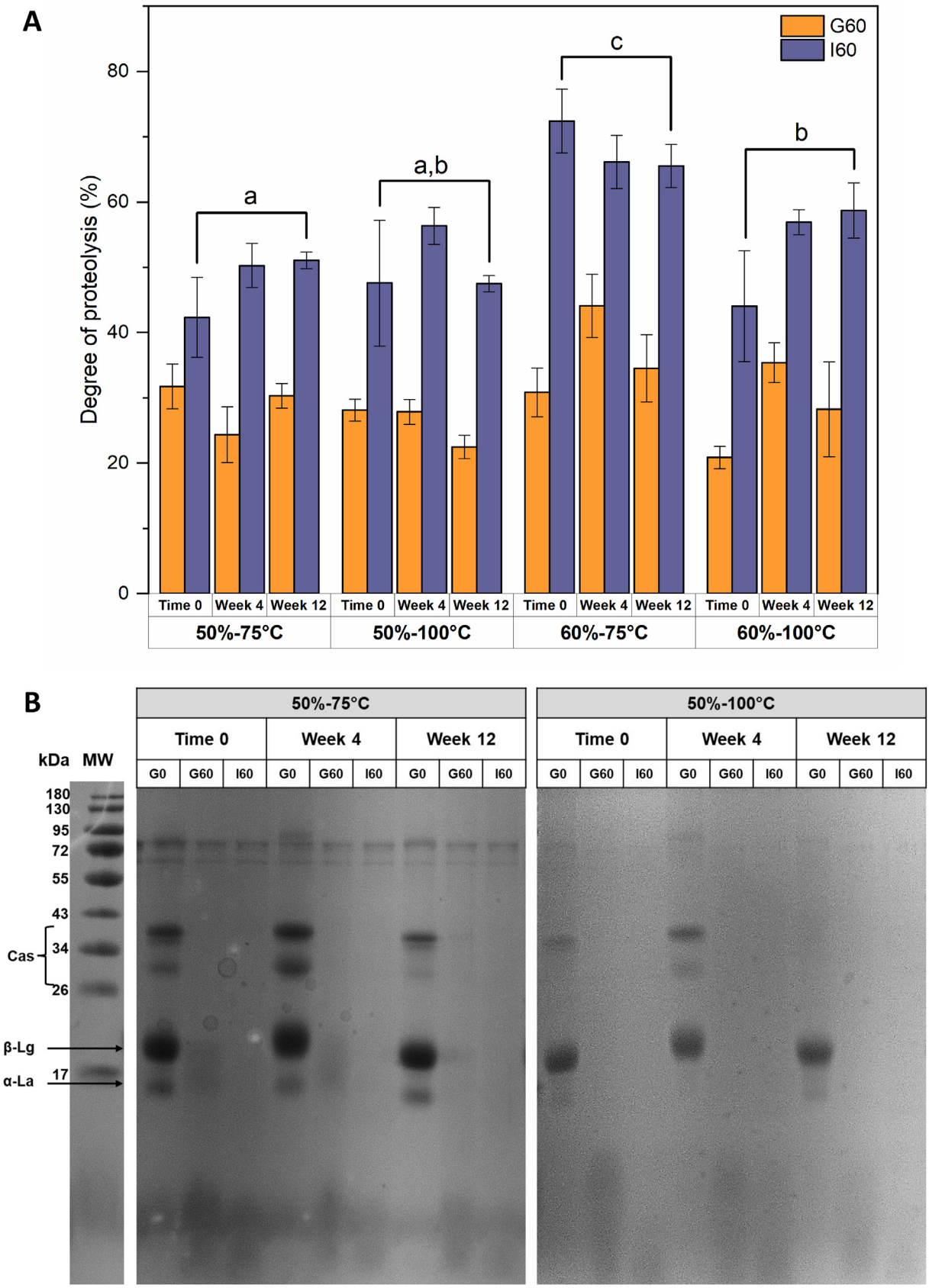

Fig. 6. Degree of proteolysis (A) and reducing-SDS-PAGE protein profiles (B) during *in vitro* static digestion of the model infant milk formulas, before storage (time 0), after 4 weeks of storage under open package conditions and after 12 weeks of storage under closed package conditions. Error bars in Fig. 6.A indicate standard deviations (n = 6). Cas = caseins, β-Lg = β-lactoglobulin and α-lactalbumin. Different lower cases indicate significant differences ($p < 0.05$) in I60 between formulas.

Table 2
Free fatty acids (g oleic acid/100 mL) released during *in vitro* gastrointestinal digestion (I60 − G0) of model infant milk formulas, before storage (time 0), after 4 weeks of storage under open package conditions and after 12 weeks of storage under closed package conditions.

IMF	Free fatty acids (g oleic acid/100 mL)		
	Time 0	Week 4	Week 12
50%-75 °C	0.56 ± 0.01^{aA}	0.70 ± 0.02^{aB}	0.82 ± 0.01^{aC}
50%-100 °C	0.74 ± 0.14^{aA}	0.84 ± 0.02^{bA}	1.00 ± 0.02^{bA}
60%-75 °C	0.67 ± 0.11^{aA}	0.68 ± 0.00^{aA}	0.95 ± 0.02^{bB}
60%-100 °C	0.74 ± 0.12^{aA}	0.73 ± 0.01^{aA}	0.92 ± 0.01^{bA}

Mean ± standard deviation (n = 6). Different lower-case letters indicate significant differences ($p < 0.05$) between formulas, for each storage time. Different upper-case letters indicate significant differences ($p < 0.05$) between storage times, for each formula.

partition of the proteins between the bulk phase and the oil-water interface, which in turn impacted the rate of hydrolysis during gastric digestion. In addition, Bourlieu et al. (2015) reported that the differences in the initial emulsion structure, i.e. droplet size and interface composition, are maintained during gastric digestion, therefore explaining why 60%-75 °C was also hydrolysed the fastest during intestinal digestion.

3.4.2. Degree of lipolysis

The concentration of FFA released during digestion (I60-G0) is shown in Table 2. The ANOVA results indicated that both the effects of the formula (or processing conditions) ($p = 0.0048$) and storage conditions ($p < 0.0001$) were significant, while the interaction Formula × Storage condition was not ($p = 0.5678$). When analysing the effect 'Formula' separately, it was found that 50%-75 °C had the lowest and 50%-100 °C the highest lipolysis, while 60%-75 °C and 60%-100 °C showed an intermediate behaviour. The oil droplet sizes of the reconstituted IMFs were analysed in a previous work (Rodríguez Arzuaga et al., 2022). The results showed that 50%-100 °C had two size populations with mean diameters of 2.3 ± 0.7 μm and 27.2 ± 3.3 μm, while 50%-75 °C had a monomodal population with a mean diameter of 4.8 ± 0.5 μm. Therefore, the higher degree of lipolysis found in 50%-100 °C compared to 50%-75 °C, by the end of intestinal digestion, cannot be explained by the initial oil droplet size. However, the degree of lipolysis is not only related to the initial oil droplet surface area, but also to the interface composition that can impact the degree of droplet aggregation after the destruction of the emulsifiers located at the interface, during the gastric phase (Liu et al., 2022). In addition, bile salts are added at the intestinal phase, with one of their key roles during digestion being to prepare the fat surface to improve the access of lipolytic enzymes (Maldonado-Valderrama, Wilde, MacIerzanka, & MacKie, 2011). As a result, only small variations in the FFA release during gastrointestinal digestion were observed between samples.

When looking at the storage effect, significant differences ($p < 0.05$) were only found in 50%-75 °C and 60%-75 °C (Table 2). For such formulas, the storage under closed package conditions resulted in the largest FFA release during the gastrointestinal digestion.

4. Conclusions

The physical stability of the IMF powders depended both on the storage (open or closed package-like conditions) and the wet-mix processing conditions (heat treatment and TS).

Major changes were observed on the macro and microscopic characteristics of the powders after two weeks of storage under open package conditions (T = 25 °C, RH = 58%). Under such storage conditions, the lactose present in the formulas crystallised completely between weeks 1 and 2, and the presence of αβ-D-lactose and α-lactose monohydrate crystals was verified in the four IMFs. Lactose crystallisation led to a considerable increase in the surface free fat content of the powders and induced caking.

The TS level of the wet mix impacted the stability of the formulas. IMFs produced from wet mixes with 60% TS presented broken particles, which increased the moisture sorption rate, therefore reducing the Tg and accelerating the lactose crystallisation and surface fat liberation in the powders.

The formulas stored under closed package conditions were stable for 12 weeks, as lactose remained in amorphous state and non-major changes were observed on the powders.

Although significant physical changes were observed in the IMFs after only two weeks of storage under open package conditions, these changes did not generate a relevant impact on their digestibility.

CRediT authorship contribution statement

Mariana Rodríguez Arzuaga: Writing − original draft, Investigation, Formal analysis, Conceptualization. **Analía G. Abraham:** Writing − review & editing, Supervision, Conceptualization. **Leopoldo Suescun:** Writing − review & editing, Investigation, Formal analysis. **Alejandra Medrano:** Writing − review & editing. **Lilia Ahrné:** Writing − review & editing, Conceptualization. **Marcela Díaz:** Investigation, Formal analysis. **Jessica Báez:** Writing − review & editing, Investigation. **María Cristina Añón:** Writing − review & editing, Supervision, Conceptualization.

Declaration of competing interest

None.

Acknowledgments

Marcela Díaz is supported by the grant 2021-240122 of Chan Zuckerberg Initiative DAF, an advised fund of the Silicon Valley Community Foundation.

Appendix A. Supplementary data

Supplementary data to this article can be found online at https://doi.org/10.1016/j.idairyj.2024.105968.

References

AOAC International. (2016). Official Method 947.05. Acidity of milk. In *Official Methods of Analysis of AOAC International* (20th ed.).

Bavaro, S. L., Mamone, G., Picariello, G., Callanan, M. J., Chen, Y., Brodkorb, A., et al. (2021). Thermal or membrane processing for infant milk formula: Effects on protein digestion and integrity of the intestinal barrier. *Food Chemistry, 347*(January). https://doi.org/10.1016/j.foodchem.2021.129019

Biliaderis, C. G., Lazaridou, A., Mavropoulos, A., & Barbayiannis, N. (2002). Water plasticization effects on crystallization behavior of lactose in a co-lyophilized amorphous polysaccharide matrix and its relevance to the glass transition. *International Journal of Food Properties, 5*(2), 463−482. https://doi.org/10.1081/JFP-120005798

Blanchard, E., Zhu, P., & Schuck, P. (2013). Infant formula powders. In *Handbook of food powders: Processes and properties* (pp. 465−483). Elsevier Inc. https://doi.org/10.1533/9780857098672.3.465.

Bourlieu, C., Ménard, O., De La Chevasnerie, A., Sams, L., Rousseau, F., Madec, M. N., et al. (2015). The structure of infant formulas impacts their lipolysis, proteolysis

and disintegration during in vitro gastric digestion. *Food Chemistry, 182*, 224–235. https://doi.org/10.1016/j.foodchem.2015.03.001
Cheng, H., Erichsen, H., Soerensen, J., Petersen, M. A., & Skibsted, L. H. (2019). Optimising water activity for storage of high lipid and high protein infant formula milk powder using multivariate analysis. *International Dairy Journal, 93*, 92–98. https://doi.org/10.1016/j.idairyj.2019.02.008
Cheng, H., Zhu, R. G., Erichsen, H., Soerensen, J., Petersen, M. A., & Skibsted, L. H. (2017). High temperature storage of infant formula milk powder for prediction of storage stability at ambient conditions. *International Dairy Journal, 73*, 166–174. https://doi.org/10.1016/j.idairyj.2017.05.007
Codex Alimentarius. (2007). *Standard for infant formula and formulas for special medical purposes intended for infants. Codex Standard 72*. Codex Alimentarius.
Drapier-Beche, N., Fanni, J., Parmentier, M., & Vilasi, M. (1997). Evaluation of lactose crystalline forms by nondestructive analysis. *Journal of Dairy Science, 80*(3), 457–463. https://doi.org/10.3168/jds.S0022-0302(97)75957-5
European Commission. (2016). *Commission Delegated Regulation (EU) 2016/127 of 25 September 2015* (pp. 1–25). Official Journal of the European Union.
Fan, F., & Roos, Y. H. (2015). X-ray diffraction analysis of lactose crystallization in freeze-dried lactose-whey protein systems. *Food Research International, 67*, 1–11. https://doi.org/10.1016/j.foodres.2014.10.023
Fries, D. C., Rao, S. T., & Sundaralingam, M. (1971). Structural chemistry of carbohydrates. III. Crystal and molecular structure of 4-O-β-D-galactopyranosyl-α-D-glucopyranose monohydrate (α-lactose monohydrate). *Acta Crystallographica Section B Structural Crystallography and Crystal Chemistry, 27*(5), 994–1005. https://doi.org/10.1107/s0567740871003364
GEA Niro. (2006). *GEA Niro Method No. A 1 a. Powder moisture accurate standard method*. https://www.gea.com/es/binaries/A_1_a-Powder_Moisture_Accurate_Standard_Method_tcm25-30900.pdf.
Groom, C. R., Bruno, I. J., Lightfoot, M. P., & Ward, S. C. (2016). The Cambridge Structural Database. *Acta Crystallographica Section B, B72*, 171–179. https://doi.org/10.1107/S2052520616003954
Guiry, K. P., Coles, S. J., Moynihan, H. A., & Lawrence, S. E. (2008). Effect of 1-deoxy-D-lactose upon the crystallization of D-lactose. *Crystal Growth & Design, 8*(11), 3927–3934. https://doi.org/10.1021/cg070598n
Halabi, A., Croguennec, T., Bouhallab, S., Dupont, D., & Deglaire, A. (2020). Modification of protein structures by altering the whey protein profile and heat treatment affects: In vitro static digestion of model infant milk formulas. *Food & Function, 11*(8), 6933–6945. https://doi.org/10.1039/d0fo01362e
Han, J., Fitzpatrick, J., Cronin, K., Maidannyk, V., & Miao, S. (2021c). Particle size, powder properties and the breakage behaviour of infant milk formula. *Journal of Food Engineering, 292*(August 2020), Article 110367. https://doi.org/10.1016/j.jfoodeng.2020.110367
Han, J., Fitzpatrick, J., Cronin, K., Maidannyk, V., & Miao, S. (2022). Breakage behaviour and functionality of spray-dried agglomerated model infant milk formula: Effect of proteins and carbohydrates content. *Food Chemistry, 391*. https://doi.org/10.1016/j.foodchem.2022.133179
Han, J., Fitzpatrick, J., Cronin, K., & Miao, S. (2021a). Dairy powder breakage: Mechanisms, characterization methods, impacted properties and influencing factors. *Trends in Food Science & Technology, 114*(August 2020), 608–624. https://doi.org/10.1016/j.tifs.2021.05.043
Han, J., Fitzpatrick, J., Cronin, K., & Miao, S. (2021b). Investigation of the influence of powder characteristics on the breakage of dairy powders. *Food Research International, 150*(PA), Article 110775. https://doi.org/10.1016/j.foodres.2021.110775
Haque, M. K., & Roos, Y. H. (2005). Crystallization and X-ray diffraction of crystals formed in water-plasticized amorphous spray-dried and freeze-dried lactose/protein mixtures. *Journal of Food Science, 70*(5), 359–366.
Hourigan, J. A., Lifran, E. V., Vu, L. T. T., Listiohadi, Y., & Sleigh, R. W. (2013). Lactose: Chemistry, processing, and utilization. In G. W. Smithers, & M. A. Augustin (Eds.), *Advances in dairy ingredients* (1st ed., pp. 31–69). John Wiley & Sons, Inc. https://doi.org/10.1002/9781118448205.
ICDD. (2013). *PDF-2 2013*. International Centre for Diffraction Data.
Jouppila, K., Kansikas, J., & Roos, Y. H. (1997). Glass transition, water plasticization, and lactose crystallization in skim milk powder. *Journal of Dairy Science, 80*(12), 3152–3160. https://doi.org/10.3168/jds.S0022-0302(97)76286-6
Jouppila, K., Kansikas, J., & Roos, Y. H. (1998). Crystallization and X-ray diffraction of crystals formed in water-plasticized amorphous lactose. *Biotechnology Progress, 14*(2), 347–350.
Kim, E. H. J., Chen, X. D., & Pearce, D. (2009). Surface composition of industrial spray-dried milk powders. 1. Development of surface composition during manufacture. *Journal of Food Engineering, 94*(2), 163–168. https://doi.org/10.1016/j.jfoodeng.2008.09.021
Kirk, J. H., Dann, S. E., & Blatchford, C. G. (2007). Lactose: A definitive guide to polymorph determination. *International Journal of Pharmaceutics, 334*(1–2), 103–114. https://doi.org/10.1016/j.ijpharm.2006.10.026
Li, X., Gu, Y., He, S., Dudu, O. E., Li, Q., Liu, H., et al. (2020). Influence of pasteurization and storage on dynamic in vitro gastric digestion of milk proteins: Quantitative insights based on peptidomics. *Foods, 9*(8). https://doi.org/10.3390/foods9080998
Liu, L., Lin, S., Ma, S., Sun, Y., Li, X., & Liang, S. (2022). A comparative analysis of lipid digestion in human milk and infant formulas based on simulated in vitro infant gastrointestinal digestion. *Foods, 11*(2). https://doi.org/10.3390/foods11020200
Macierzanka, A., Sancho, A. I., Mills, E. N. C., Rigby, N. M., & MacKie, A. R. (2009). Emulsification alters simulated gastrointestinal proteolysis of β-casein and β-lactoglobulin. *Soft Matter, 5*(3), 538–550. https://doi.org/10.1039/b811233a
Maldonado-Valderrama, J., Wilde, P., Maclerzanka, A., & MacKie, A. (2011). The role of bile salts in digestion. *Advances in Colloid and Interface Science, 165*(1), 36–46. https://doi.org/10.1016/j.cis.2010.12.002
Masum, A. K. M., Chandrapala, J., Huppertz, T., Adhikari, B., & Zisu, B. (2020a). Effect of storage conditions on the physicochemical properties of infant milk formula powders containing different lactose-to-maltodextrin ratios. *Food Chemistry, 319*(March). https://doi.org/10.1016/j.foodchem.2020.126591
Masum, A. K. M., Chandrapala, J., Huppertz, T., Adhikari, B., & Zisu, B. (2020b). Influence of drying temperatures and storage parameters on the physicochemical properties of spray-dried infant milk formula powders. *International Dairy Journal, 105*. https://doi.org/10.1016/j.idairyj.2020.104696
McCarthy, N. A., Gee, V. L., Hickey, D. K., Kelly, A. L., O'Mahony, J. A., & Fenelon, M. A. (2013). Effect of protein content on the physical stability and microstructure of a model infant formula. *International Dairy Journal, 29*(1), 53–59. https://doi.org/10.1016/j.idairyj.2012.10.004
Ménard, O., Bourlieu, C., De Oliveira, S. C., Dellarosa, N., Laghi, L., Carrière, F., Capozzi, F., Dupont, D., & Deglaire, A. (2018). A first step towards a consensus static in vitro model for simulating full-term infant digestion. *Food Chemistry, 240*(July 2017), 338–345. https://doi.org/10.1016/j.foodchem.2017.07.145
Miao, S., & Roos, Y. H. (2005). Crystallization kinetics and X-ray diffraction of crystals formed in amorphous lactose, trehalose, and lactose/trehalose mixtures. *Journal of Food Science, 70*(5), 350–358. https://doi.org/10.1111/j.1365-2621.2005.tb09976.x
Montagne, D.-H., Van Dael, P., Skanderby, M., & Hugelshofer, W. (2009). Infant formulae - Powders and liquids. In A. Y. Tamime (Ed.), *Dairy powders and concentrated products* (pp. 294–331). Blackwell Publishing Ltd. https://doi.org/10.1002/9781444322729.ch9.
Murrieta-Pazos, I., Gaiani, C., Galet, L., Cuq, B., Desobry, S., & Scher, J. (2011). Comparative study of particle structure evolution during water sorption: Skim and whole milk powders. *Colloids and Surfaces B: Biointerfaces, 87*(1), 1–10. https://doi.org/10.1016/j.colsurfb.2011.05.001
Nielsen, P. M., Petersen, D., & Dambmann, C. (2001). Improved method for determining food protein degree of hydrolysis. *Journal of Food Science, 66*(5), 642–646.
Nijdam, J., Ibach, A., Eichhorn, K., & Kind, M. (2007). An X-ray diffraction analysis of crystallised whey and whey-permeate powders. *Carbohydrate Research, 342*(16), 2354–2364. https://doi.org/10.1016/j.carres.2007.08.001
Palzer, S. (2010). The relation between material properties and supra-molecular structure of water-soluble food solids. *Trends in Food Science and Technology, 21*(1), 12–25. https://doi.org/10.1016/j.tifs.2009.08.005
Patil, M. H., Tanguy, G., Le Floch-Fouéré, C., Jeantet, R., & Murphy, E. G. (2021). Energy usage in the manufacture of dairy powders: Advances in conventional processing and disruptive technologies. *Drying Technology, 39*(11), 1595–1613. https://doi.org/10.1080/07373937.2021.1903489
Rietveld, H. M. (1969). A profile refinement method for nuclear and magnetic structures. *Journal of Applied Crystallography, 2*, 65–71. https://doi.org/10.1107/S0021889869006558
Rodríguez Arzuaga, M., Aalaei, K., Felix da Silva, D., Barjon, S., Abraham, A. G., Añón, M. C., et al. (2021a). Infant milk formulae processing: Effect of wet-mix total solids and heat treatment temperature on rheological, emulsifying and nutritional properties. *Journal of Food Engineering, 290*. https://doi.org/10.1016/j.jfoodeng.2020.110194
Rodríguez Arzuaga, M., Abraham, A. G., Ahrné, L., Pérez Montes, M. G., & Añón, M. C. (2022). Spray-dried infant formula emulsion stability as affected by pre-heat treatment and total solids content of the feed. *Foods, 11*(23), 1–14. https://doi.org/10.3390/foods11233752
Rodríguez Arzuaga, M., Felix da Silva, D., Xanthakis, E., Aalaei, K., Czaja, T. P., Añón, M. C., et al. (2021b). Impact of wet-mix total solids content and heat treatment on physicochemical and techno-functional properties of infant milk formula powders. *Powder Technology, 390*, 473–481. https://doi.org/10.1016/j.powtec.2021.05.093
Saffari, M., & Langrish, T. (2014). Effect of lactic acid in-process crystallization of lactose/protein powders during spray drying. *Journal of Food Engineering, 137*, 88–94. https://doi.org/10.1016/j.jfoodeng.2014.04.002
Sangeetha, M. K., Mariappan, M., Madhurambal, G., & Mojumdar, S. C. (2015). TG-DTA, XRD, SEM, EDX, UV, and FT-IR spectroscopic studies of l-valine thiourea mixed crystal. *Journal of Thermal Analysis and Calorimetry, 119*(2), 907–913. https://doi.org/10.1007/s10973-014-4123-6
Saxena, J., Adhikari, B., Brkljaca, R., Huppertz, T., & Chandrapala, J. (2020). Interrelationship between lactose crystallization and surface free fat during storage of infant formula. *Food Chemistry, 322*(February), Article 126636. https://doi.org/10.1016/j.foodchem.2020.126636
Saxena, J., Adhikari, B., Brkljaca, R., Huppertz, T., Zisu, B., & Chandrapala, J. (2021). Effect of compositional variation on physico-chemical and structural changes in infant formula during storage. *International Dairy Journal, 116*(104957), Article 104957. https://doi.org/10.1016/j.idairyj.2020.104957

Simpson, T. D., Parrish, F. W., & Nelson, M. L. (1982). Crystalline forms of lactose produced in acidic alcoholic media. *Journal of Food Science, 47*(6), 1948–1951. https://doi.org/10.1111/j.1365-2621.1982.tb12920.x

Tham, T. W. Y., Wang, C., Yeoh, A. T. H., & Zhou, W. (2016). Moisture sorption isotherm and caking properties of infant formulas. *Journal of Food Engineering, 175*, 117–126. https://doi.org/10.1016/j.jfoodeng.2015.12.014

Tham, T. W. Y., Xu, X., Yeoh, A. T. H., & Zhou, W. (2017a). Investigation of caking by fat bridging in aged infant formula. *Food Chemistry, 218*, 30–39. https://doi.org/10.1016/j.foodchem.2016.09.043

Tham, T. W. Y., Yeoh, A. T. H., & Zhou, W. (2017b). Characterisation of aged infant formulas and physicochemical changes. *Food Chemistry, 219*, 117–125. https://doi.org/10.1016/j.foodchem.2016.09.107

Toby, B. H., & Von Dreele, R. B. (2013). GSAS-II: The genesis of a modern open-source all purpose crystallography software package. *Journal of Applied Crystallography, 46*, 544–549. https://doi.org/10.1107/S0021889813003531

Vega, C., Douglas Goff, H., & Roos, Y. H. (2007). Casein molecular assembly affects the properties of milk fat emulsions encapsulated in lactose or trehalose matrices. *International Dairy Journal, 17*(6), 683–695. https://doi.org/10.1016/j.idairyj.2006.08.004

Vignolles, M. L., Jeantet, R., Lopez, C., & Schuck, P. (2007). Free fat, surface fat and dairy powders: Interactions between process and product. A review. *Le Lait, 87*(3), 187–236. https://doi.org/10.1051/lait:2007010